A 1,5 kW FB-ZVS-PWM CONVERTER APPLIED TO FUEL CELL SYSTEMS

M. A. Pagliosa*, Y. R. de Novaes** and I. Barbi**
* University of the West of Santa Catarina – UNOESC, Graduate Course of Electrical Engineering, Rua Getúlio Vargas 2125
89600-000 - Joaçaba – SC- Brazil
** Federal University of Santa Catarina – UFSC, Institute of Power Electronics - INEP, Po. Box 5119
88040-970 - Florianópolis - SC - Brazil
e-mail: mauro.pagliosa@unoesc.edu.br

Abstract -**This paper presents a design for a 1.5kW Full-Bridge Zero-Voltage Switching Pulse-Width modulation converter, using a fuel cell (FC) as input energy source. The study starts explaining the FC working principle and electrical behavior. The requirement of converter operation, determined by electrical behavior of the FC, with high current levels at high frequency, makes the parasite inductance effects relevant on the electrical circuit. Thus, parameters commonly overlooked to the mathematical analysis must be considered. Such effects were analyzed through numerical simulation and attested to in the experimental results.**

Keywords – **Converter, Fuel Cell, Soft-Switching, Stray Inductance.**

I. INTRODUCTION

The Fuel Cell (FC), as a promising energy conversion mechanism, combines hydrogen and oxygen to produce electricity, with water and heat as its by-products. As the conversion of the fuel to energy takes place via an electrochemical process, the process is clean, quiet and more efficient than burning fuel. In addition to low or zero emissions, benefits will also include high efficiency, reliability and multi-fuel capacity. Since FCs operate silently, they reduce noise pollution as well as air pollution allowing the waste heat of a fuel cell to be used to provide hot water or home/office space heating.

Motivated by this promising FC application, this paper presents a Full-Bridge, Zero-voltage Switching, Pulse-Width-Modulation (FB-ZVS-PWM) converter, applied to a Proton Exchanged Membrane Fuel Cell (PEMFC). The power produced is 1.5kW, output voltage is adjustable between 48V and 60V, output current will be controlled for use with rechargeable batteries. Input voltage is determined by electrical behavior of PEMFC, 24 to 36V. These input voltage levels with 1.5kW and high frequency current produce, by experimental results, some undesired effects caused by stray inductions and transformer leakage inductance.

II. THE FUEL CELL

A fuel cell converts the chemical hydrogen and oxygen into water, electricity and heat. These chemical processes determine the static and dynamic electrical behavior of the FC [1]-[4].

A. Fuel Cell Static behavior: There are basically three distinct regions that govern the static fuel cell voltage behavior. Figure 1 presents the theoretical voltage behavior as current function.

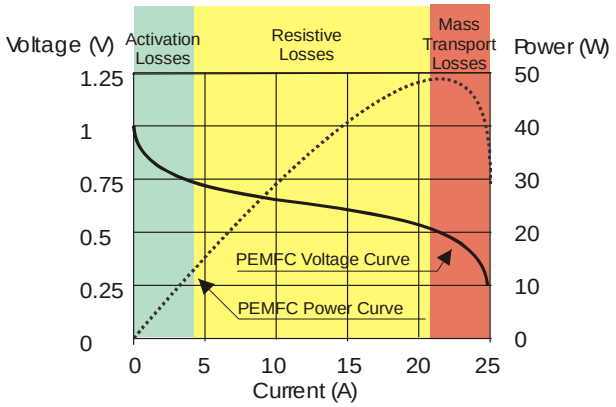

Fig. 1 Static Behavior.

The first and very pronounced voltage drop is due to the activation losses related to the reactions taking place on the surface of the electrode [4]. The second voltage drop can be considered linear and represents the resistance of the electrolyte against electron or ion circulation. At the end of the curve, the mass (reactants) transport losses are represented by another quick voltage drop. This is the point of maximum fuel cell power output. Afterwards, the efficiency of the fuel cell decreases rapidly and, for this reason, is not usually surpassed. There is also another phenomenon named gas crossing that produces some gas circulation through the membrane, resulting finally in a small reduction in the fuel cell open voltage [4].

The parameters obtained are important in order to evaluate the fuel cell influence in output characteristics of the static converter, especially when the fuel cell operates in the linear region as shown by the graph.

B. Fuel Cell Dynamic Behavior: Figure 2 represents an electrical fuel cell dynamic model. For each step in current variation, there would be a corresponding step in voltage variation proportional to resistor R_{ohm} and an exponential variation due to components R_{act} and C_{act} [4]. This present work produced the dynamic behavior parameter by current interruption method, which consists of interrupting the current and measuring the voltage waveform at a certain fuel cell operating point. From this method, the 1.5 kW PEMFC parameters are represented by (1), (2) and (3) [5].

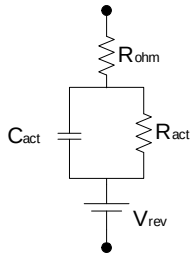

Fig. 2 – Electrical fuel cell dynamic model.

$$R_{ohm} = 0{,}180\Omega \quad (1)$$

$$R_{act} = 0{,}832\Omega \quad (2)$$

$$C_{act} = 0{,}07F \quad (3)$$

The ripple current can contribute to a reduction in the fuel cell available output power, cause internal losses, and increase distortion of its terminal voltage [6]. The capacitor C_{act} on figure 2, suggest that this effects can be reduced when the ripple frequency increase.

III. A 1,5 KW ISOLATED DC-DC CONVERTER ARCHITECTURE

Systems based only on batteries do not provide sufficient backup power to supply critical loads. Hence, another energy source or storage technology must be used to increase the autonomy of the entire system. The system present here based on fuel cells which can provide long-term backup power.

The FB-ZVS-PWM converter is used to process the 1.5kW generated by a PEMFC. A rechargeable battery is connected at the converter output along with the charge. This battery will be used to supply the charge during the fuel cell warm-up time. After the warm-up, the converter will charge the battery and supply the load. The input source is composed of six fuel cell stacks connected in parallel and each stack is composed of 48 cells connected in series. Figure 3 shows the connection schematics and Figure 4 shows the converter architecture [7]-[8].

The PEMFC ripple current is reduced by the connection of a capacitor filter between the PEMFC and the converter.

A. DC-DC converter specifications

Converter parameter specification is on Table I. Input voltage is determined by the static behavior of the PEMFC

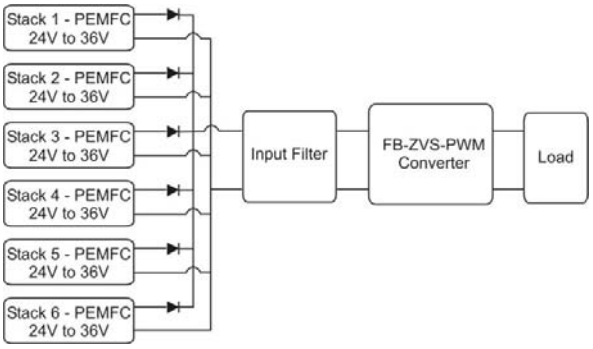

Fig. 3 PEMFC Stacks and Converter Connection Schematic Diagram

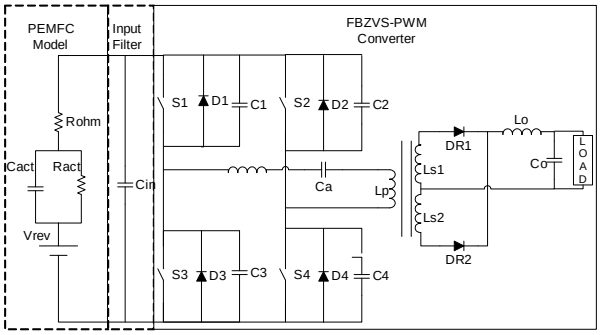

Fig. 4 Electrical circuit connection.

TABLE I
Converter Operation Specification

Specification	Value
Input voltage	$24V_{DC}$ to $36V_{DC}$
Output voltage	$48V_{DC}$ to $60V_{DC}$ (adjustable)
Output Power	1,5kW
Frequency switching	40kHz
Duty Cycle Loss	15%
Output Ripple Current	5%
Output Ripple Voltage	10%
Power Efficiency	80%
Turns Ratio of Transformer	N_1:N_2 = 1:4

Table II shows the converter parameter operation calculated from Table I data.

TABLE II
Calculated Converted Parameter

Parameters	Value
Load Current	$I_{o\_max} = 31{,}25A_{RMS}$
Secondary Transformer Current	$I_{sec\_1} = I_{sec\_2} = 22{,}09A_{RMS}$
Primary Transformer Current	$I_{prim} = 125A_{RMS}$
Resonant Inductor Current	$I_{Lr} = 125A_{RMS}$
Fuel Cell Current	$I_{CaC} = 75A_{RMS}$
Effective Duty Cycle	$D_{ef} = 0{,}75$
Switching S1 and S3 current	$I_{ef\_s1\_s3} = 77A_{RMS}$
Switching S2 and S4 current	$I_{ef\_s2\_s4} = 82{,}6A_{RMS}$
Resonant Inductance	$L_R = 162\eta H$
Current on the Input Capacitor Filter	$Ic_{in} = 56A_{RMS}$

At the design of the circuit of the converter, the resultant difficulties are evident in operating a converter with elevated current levels at high frequency. The difficulties are related especially to the high peak voltage at the switches and a drop in the duty cycle, parameters that are directly affected by the stray inductances of the circuit.

As it is not possible to predict stray inductance values with precision, since it would depend on converter construction aspects, the dimensioning of the elements which compose the converter power stage is initially done thorough the mathematical analyses of operational mode, considering an idealized mode of operation. At the second phase, the switch inductances provided by the manufacturer are introduced into the simulation circuit. The results of the simulation, for this case, indicate the need to reduce the voltage peaks in the power switches.

The first solution proposed by this work was to increase the intrinsic capacitance of the switches, adding external capacitors in a way to reduce the voltage derivative at the moment of switch off, thus reducing the peak at the mentioned voltage. The value of the capacitors in parallel with the switches were defined by the resonant switching step time, which has a value of 1us, resulting in 2uF of capacitance. Although this solution had resolved the problem related to the voltage peaks in the switches, the current circulating among the externally added capacitors would reach 30A, making implementation difficult due to the low current capacity of the commercially available capacitors.

A viable alternative was to add Schottcky diodes in antiparallel to the switches, such that their voltage would not surpass the coded value. This solution allowed the switch voltage to remain within the operational limits of the component, and the current that was previously too elevated in the commutating capacitors could diminish due to distribution among the externally added diodes. The simulation results on the value of the current in the commutating capacitor reduced from 30A to 12A.

On the converter input filter, four capacitors in parallel, able to support 56A of current, were associated (as observed on Table II). This association results in a total input capacity of 16000µF. When this value is compared to the electrical dynamic fuel cell model described above, it can be concluded that filter capacitance cancels out the fuel cell dynamic behavior on the converter's electrical characteristics. As a result, an ideal input voltage source can be used instead of the electrical fuel cell model on the small-signal ac model of the converter. The simulation result was used to confirm the condition described above. Figure 5 presents the equivalent implemented circuit of converter.

The transformer is also a critical element in the converter design as the inductance leakage in the primary side must be inferior to the maximum of the resonant inductance. As the calculated resonant inductance is low, the transformer will require a precise care in assembling to reduce the leakage inductance value as much as possible on the primary side. The inductance leakage of the assembled transformer on this project was 130ηH, thus being below the maximum limit of the resonant inductor value. A common characteristic in the design of the FB-ZVS-PWM converter is to determine the range of soft-switching in which it may operate. In the study case, due to the low value of calculated resonant inductance, the major concern is to guarantee the static gain necessary to the nominal operation power.

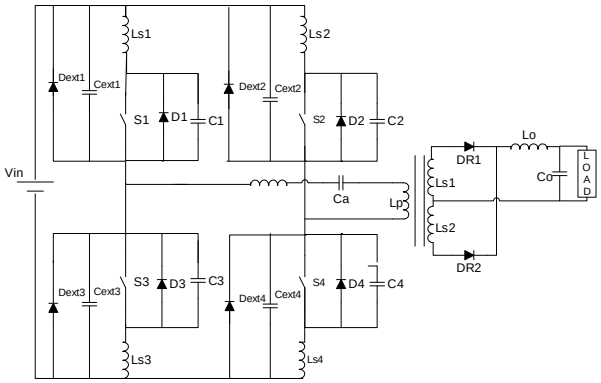

Fig. 5 Equivalent implemented circuit.

Where:
D_{ext}1,2,3 and 4 - External Shotticky diode included;
C_{ext}1,2,3 and 4 - External Capacitor included;
L_s1,2,3 and 4 - Stray inductance;

An inrush current circuit was used at the converter's input to limit the current during the start up procedure.

B. DC-DC converter control stage

The converter output voltage is stabilized and adjustable from 48V to 60V by means of a voltage feedback controller. The output converter current is limited by the current feedback controller working in parallel with the voltage controller. This limited current is used for protection of converter operation and battery charging. Both controllers used are analog Proportional, Integrate and Derivative Controllers (PID). Figure 6 presents the converter feedback control system schematic diagram, where the current and voltage controllers are working in parallel connected by diode. The diode function is to select one of these controllers, just one of controllers can work at the same time, become independent each other.

The voltage and current converter transfer functions are shown on (3) and (4) [9].

$$\frac{V_o(s)}{D(s)} = \frac{n.V_i}{R_\sigma} \cdot \frac{C_o.R_{SE}.S+1}{L_o.C_o.\left(1+\frac{R_{SE}}{R_o}\right).S^2 + \left(C_o.R_{SE}.4.n^2.L_r.f + \frac{L_o}{R_o}\right).S + \frac{4.n^2.L_r.f}{R_o}+1} \quad (3)$$

$$\frac{I_L(s)}{D(s)} = \frac{n.V_i.R_o}{R_\sigma} \cdot \frac{C_o.R_{SE}.S+1}{L_o.C_o.\left(1+\frac{R_{SE}}{R_o}\right).S^2 + \left(C_o.R_{SE}.4.n^2.L_r.f + \frac{L_o}{R_o}\right).S + \frac{4.n^2.L_r.f}{R_o}+1} \quad (4)$$

Where R_σ is represented by (5)

$$R_\sigma = \frac{4.n^2.L_r.f}{R_o} + 1 \quad (5)$$

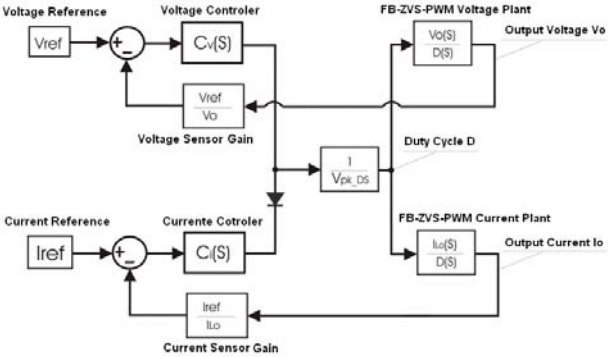

Fig. 6 Converter Control System.

IV. EXPERIMENTAL RESULTS

Figure 7 shows the converter output voltage is stabilized to step load. Figure 8 shows the current is limited by current controller. As a result, output voltage drops as load increases.

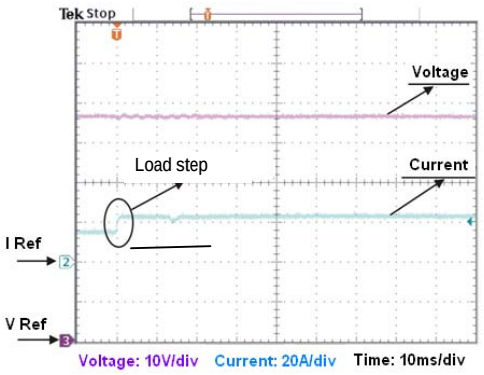

Fig. 7 Converter output voltage curve and current curve for load step.

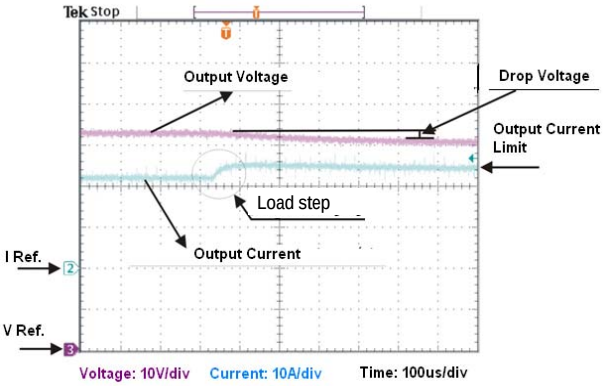

Fig. 8 Converter output voltage curve and current curve by time for load step.

The soft-switching can be observed in Figure 9 where the switching voltage and switching signal command are shown.

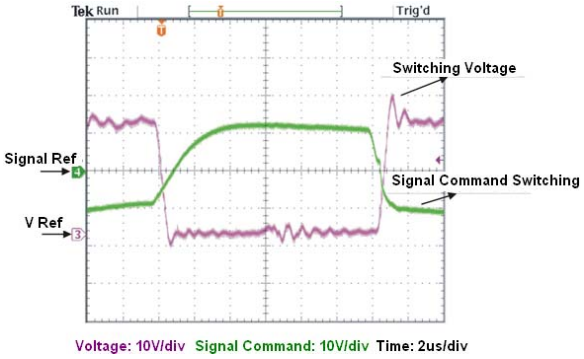

Fig. 9 Switching voltage curve and switching signal command curve.

Figure 10 shows the current on the transformer's primary side. It can be concluded that the leakage inductance value on the circuit was enough to reduce the effective duty cycle. In other words, the calculated resonant inductance was of a lower value than the inductance leakage plus transformer inductance leakage. In order to compensate the lower value of effective duty cycle, the nominal duty cycle needs to be increased, however, should a step up converter operation be considered, there will not be sufficient surplus duty cycle range. Another solution could be to change the transformer turns ratio, although this choice will increase the transformer's leakage inductance and, consequently, reduce the duty cycle again.

Within this project, as a consequence to the low effective duty cycle, the converter operates with duty cycle very close to the maximum allowed, for nominal power. Therefore, for a higher power specification than that used within the project, probably the FB-ZVS-PWM output voltage would stay under the specified value, thus making the use of such a topology quite difficult to achieve.

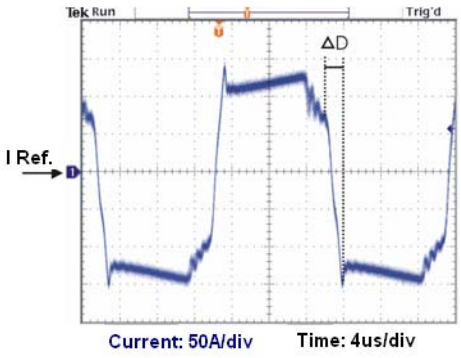

Fig. 10 Primary transformer current curve.

Figure 11 shows two measuring points where point A is the PEMFC voltage and point B the input voltage converter. Without considering the leakage inductance from the cooper wire and electrical circuit connectors, these two measuring points would be the same electrical point. The leakage inductance on the input voltage link converter is represented by the electric scheme shown on Figure 12.

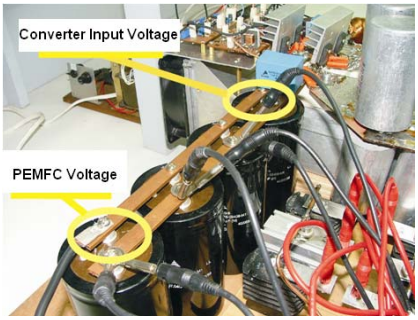

Fig. 11 Two Measuring Points of Input Voltage Converter.

The converter's input voltage, measured at point B, has more distortion when compared to point A as observed on Figures 13 and 14. This voltage distortion is important in the consideration of inductance leakage on the converter's designed step. The distortion of the converter's input voltage appears on switching and can make it difficult to control the output voltage.

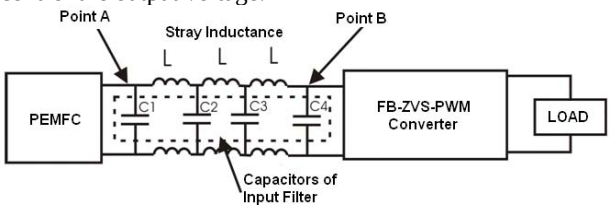

Fig. 12 Representative Electrical Circuit of Input Voltage Converter with Leakage Inductance.

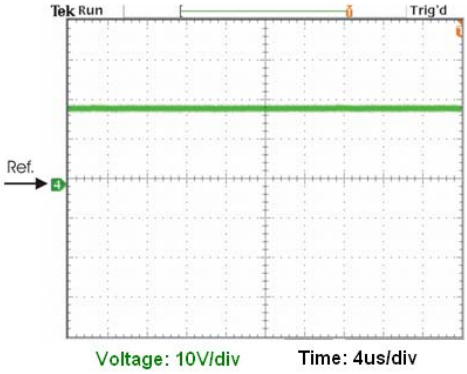

Fig. 13 Voltage curve of PEMFC (point A).

Figure 15 shows the efficiency of the FB-ZVS-PWM. For low power, efficiency is close to 90%, however, increases to 96% when the soft-switching is attained at 500W. Although the converter is on the soft-switching operating region for higher power than 500W, the switching loss is not significant when compared to Joule loss. High Joule losses are caused by high current and low voltage converter operation, and are determined by PEMFC static behavior.

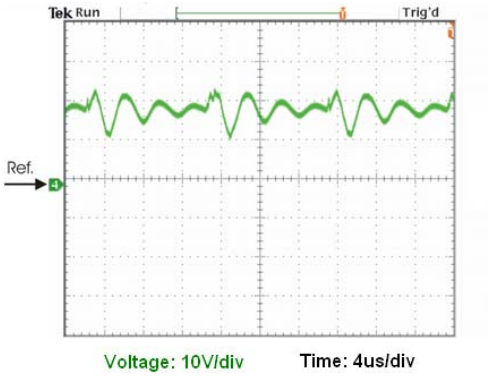

Fig. 14 Converter input voltage (point B).

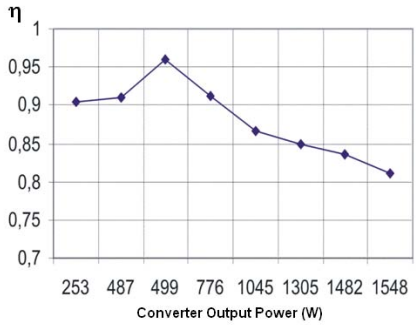

Fig. 15 Efficiency of converter vs. output power.

Where:
η = efficiency.

V. CONCLUSION

Regarding FB-ZVS-PWM converter function, it will be noted that the high current to which it is submitted in order to operate with PEMFC, will bring to light implications that may make the project unviable should the value of the calculated resonant induction is of the same order as the inductance leakage of the transformer added to inductance leakage from the circuit. The experimental results have shown that the value of the resonant inductor was quite altered by the inductance leakage, making the losses of the duty cycle higher than those foreseen in the project and, consequently, for nominal power the converter operates close to the maximum duty cycle, limiting the static voltage gain of converter.

Another effect shown by the elevated level in high frequency of the current on the converter are the voltage peaks at the switches caused by the resonance between the inductance leakage and the intrinsic capacity of the switches; the solution to this problem was obtained by simulation including capacitors and diodes in the circuit in an adequate configuration.

Considering the difficulties presented in this study, it is suggested that for the operating conditions to which the converter is submitted, the use of another converter topology such as Boost converter, for example, or the use of parallelism between two or three FB-ZVS-PWM converters with lower power.

ACKNOWLEDGEMENT

The authors gratefully acknowledge AZEGO Technology Services, and CAPES for the financial support.

REFERENCES

[1] K. Kordesch and R. F. Sproull, Fuel Cells and Their Applications. Federal Republic of Germany-Weinheim: VCH Verlagsgesellschaft, 1996.
[2] M. W. Breiter, Electrochemical Processes in Fuel Cells. Springer-Verlag Berlin, 1969.
[3] A. B. Hart and G. J. Womack, Fuel Cells Theory and Applications. Chapman and Hall Ltd, 1967.
[4] J. Larminie and A. Dicks, Fuel Cell Systems Explained. John Wiley e Sons Ltd, 2000.
[5] L. A. Serpa, Y. R. Novaes, and I. Barbi, Experimental Parametrization of Steady-State and Dynamic Models Represented by an Electrical Circuit of PEM Fuel Cell. COBEP 2003, 2003.
[6] Woojin Choi, Gyubum Joung, Prasad N. Enjeti, and Jo W. Howze; “An Experimental Evaluation of the Effects of Ripple Current Generated by the Power Conditioning Stage on a Proton Exchange Membrane Fuel Cell Stack”; Journal of Materials Engineering and Performance, vol 13, june 2004.
[7] G. Fontes, C. Turpin, R. Saisset, T. Meynard, and S. Astier, Interactions between fuel cells and power converters Influence of current harmonics on a fuel cell stack. Proceedings: IEEE Power Electronics Specialists Conference-PESC, 2004.
[8] BARBI, I.; SOUZA, F. P. de;”Conversores CC-CC Isolados de Alta Freqüência com Comutação Suave”, Edição dos Autores, 1999
[9] Vlatkovic V., Sabaté J. A., Ridley R.B., Lee F. C. and Cho B. H.; “Small-Signal Analysis of the Zero-Voltage-Switched, Full-Bridge PWM Converter”, Proceedings of the High Frequency Power Conversion Conference; Santa Clara, CA, May 6-11, 1990; pp. 262-272.